

**Study of the coronal heating in the presence
of shear flow: A numerical approach.**

B. P. Pandey¹, S. Parhi¹, **G. S. Lakhina**²,
M. Goossens³, R. DeVore⁴ and B. T. Tsurutani²

¹ Indian Institute of Geomagnetism,
Bombay 400005, India.

² Jet Propulsion Laboratory,
California Institute of Technology,
Pasadena, CA 91109, USA

³ Center for Plasma Astrophysica,
Katholic University of Leuven,
Celestijnenlaan 200B, Leuven 3001, Belgium

⁴ Laboratory for Computational Physics and Fluid Dynamics,
Naval Research Laboratory, Washington DC 20375, USA

ABSTRACT

We numerically simulate the effect of shear flow on the evolution of MHD waves in the solar corona which is modeled by a low- β , resistive plasma slab. The hydromagnetic waves are generated in the coronal loop by applying a periodic driver which mimics foot point motion in the photosphere. We detect some signatures of the kink instability and traces of logarithmic singularities at early stage of the evolution. Further temporal evolution completely removes the singularities. We infer that the flow inhibits the development of kink instability. We find that the presence of flow facilitates heating. The inclusion of a small non-zero V_y (V_y being the component of flow along the height of the loop) has tremendous effect on resonance absorption, as large changes occur in vortex structures. The center of the simulation loop consists of elongated plasma vortices, which suggests that it may break down on further evolution, The microstructure are the possible signatures of the direct cascade of energy. The direct correlation between vortex formation and the heating pattern is explained. The flow brings more or less symmetric distribution of heating.

1 Introduction

It is believed that most of the astrophysical objects (e.g., stars, accretion disks etc.) possess a hot corona. The corona is a stretched magnetic tube filled with a low density ionized gas. It has closed as well as open field topologies. It can support a variety of waves generated by convective upwelling motion in the photosphere. The corona acts as a site of wave emission as well, for example, radio, microwave, and x-ray emissions are all emanated from the sun. In order to explain the observed coronal temperature profile, resonant absorption of MHD waves by coronal plasma has been proposed as a possible candidate [(Ionson, 1978). The simple physical picture is that the footpoint motion in the photosphere constantly stirs the coronal plasma leading to the MHD wave generation which is then resonantly absorbed resulting in the enhanced heating of the corona. A general disturbance in the photosphere can produce **Alfven**, fast and slow magnetosonic waves as well as the formation of current sheets (Priest, 1981; Karpen *et al.*, 1991). For sufficiently slow photospheric motions ($\tau_A = L/V_A < \tau$, where τ_A is the Alfvén time scale, L is the size of the system, V_A is the typical Alfvén velocity and τ is the characteristic time of the photospheric motions), current sheets may play an important role in the coronal heating. A current sheet is formed by the photospheric disturbances which may bring the **topologically** separate parts of the magnetic configuration adjacent to each other. During the disruption of a current sheet, magnetic energy is released via reconnection. The temporal and spatial scale of the footpoint motion is comparable to that of the granules (Choudhuri et al, 1993a, 1993b). The new magnetic flux emerging from below the photosphere interacts with the plasma and the fields already existing at the sun. The convective motion slowly deforms the magnetic field lines which finally give rise to different topological features like loops and arcades. These morphological features can persist for days, except for occasional fast deformation in some rapid events like solar flares, etc.

Prior studies of the resonance absorption of MHD waves in an inhomogeneous plasma

in the context of solar coronal heating has been carried out by several authors (Poedts et al, 1989; Hollweg 1981, 1990; Goossens, 1991; Goossens et al 1995; Cadez and Ballester, 1994; Erdelyi and Goossens, 1994; Parhi et al, 1996a, 1996b, 1996c and references therein). It is known that Alfvén waves possess a continuous spectrum and therefore, can play a dominant role in the heating of the coronal plasma. In an inhomogeneous plasma, a nonlinear Alfvén wave can decay into a magnetosonic wave which is easily dissipated in the corona. However, the full nonlinear problem can only be studied numerically. Such a study has recently been undertaken (Parhi et al., 1996a, 1996 b). These studies were confined to a case where the background plasma had no bulk shear flow. A realistic model should deal with the presence of an equilibrium flow. The present work assumes such a non-zero bulk shear flow in the solar plasma and investigate its effect on the evolution of the waves and the heating of the corona. The analytical studies of the effect of velocity shear on resonance heating have been carried out by Hollweg et al (1990) and Yang and Hollweg (1991). They found that depending upon the values of velocity shear, absorption of waves may be enhanced or reduced. Hollweg et al (1990) concluded that the presence of the shear flow is, in general, important for the resonance heating of the corona. However, their conclusion is valid only for an incompressible fluid. Here we relax the assumption of incompressibility, and treat the solar atmosphere as compressible, which is a more realistic case. We find that the remnant of the fast wave singularity which is present in the absence of an equilibrium flow (Parhi et al, 1996a, 1996b), disappears in the presence of flow. This implies enhanced conversion of wave energy into thermal energy and thus an increased coronal temperature. This is in agreement with the conclusions of Hollweg et al (1990) and Yang and Hollweg (1991).

The plan of the paper is as follows. In section II we discuss the basic equations. In section III we describe our simulation model. The section IV discusses the simulation results. The results are summarized in section V.

2 Governing equations and basic profiles

The coronal plasma in cartesian geometry obeys the following compressible, time-dependent, resistive equations:

$$\frac{\partial \rho}{\partial t} + \nabla \cdot (\rho \mathbf{V}) = 0, \quad (1)$$

$$\frac{\partial(\rho \mathbf{V})}{\partial t} + \nabla \cdot [(\rho \mathbf{V}) \mathbf{V}] = -\nabla p + \frac{1}{\mu} (\nabla \times \mathbf{B}) \times \mathbf{B}, \quad (2)$$

$$\frac{\partial \mathbf{B}}{\partial t} = \nabla \times (\mathbf{V} \times \mathbf{B}) - \nabla \times (\eta \nabla \times \mathbf{B}), \quad (3)$$

$$\frac{\partial e}{\partial t} + \nabla \cdot (e \mathbf{V}) = -p \nabla \cdot \mathbf{V} + \frac{\eta}{\mu} (\nabla \times \mathbf{B})^2, \quad (4)$$

$$\nabla \cdot \mathbf{B} = 0. \quad (5)$$

Here ρ is the gas density, \mathbf{V} is the velocity, μ is the magnetic permeability, p is the gas pressure, \mathbf{B} is the magnetic field, $e = p/(\gamma - 1)$ is the internal energy per unit volume, η is the magnetic diffusivity and γ , the ratio of specific heats, is 5/3.

We consider a simple coronal loop modelled by a slab. The y direction is along the height of the loop, the z direction corresponds to the azimuthal direction and the inhomogeneity occurs in the x direction, corresponding to the direction of the width of the loop. We assume that the derivative of all the quantities with respect to z , i.e., $\partial/\partial z$, vanishes but V_z and B_z , the z components of perturbed flow and magnetic field, are nonzero. Consequently, both Alfvén and cusp singularities are present in such a plasma which have been recently studied by Murawski and Goossens (1994a) and Parhi and Lakhina (1994). The equilibrium density $\rho_0(x)$ and the magnetic field $B_{0y}(x)$ along the y direction are as follows:

$$\rho_0(x) = \begin{cases} \rho_i, & |x| \leq a, \\ \rho_e + (\rho_i/\rho_e - 1)\rho_e/\cosh^{14}(|x| - a), & |x| > a, \end{cases}$$

$$B_{0y}(x) = \begin{cases} B_i, & |x| \leq a, \\ B_e + (B_i/B_e - 1) B_e / \cosh^{14}(|x| - a), & |x| > a, \end{cases}$$

where the indices i and e denote the quantities inside and external to the slab, respectively. $p_0(x)$ is a smeared top-hat profile. Note that the smearing starts just at the slab edges $x = \pm a$ where a is normalized by the typical coronal loop radius (or half-width in our case) $L \sim 10^3$ km at the photosphere. The magnetic field $B_{0z}(x)$ along the z direction is taken as follows:

$$B_{0z}(x) = c e^{-c|x|}, \quad (6)$$

where c is an amplitude factor to be chosen. The plasma undergoes twist due to this magnetic field. The expression for the equilibrium gas pressure in the external region $p_{0e}(x)$ is derived from the equilibrium condition $p + B_0^2/2\mu = \text{const}$. In the region inside the slab, we consider $B_0 \sim 0.1$ T, $T_0 \sim 10^4$ K, and $n_0 \sim 10^{21} \text{ m}^{-3}$ which gives a plasma β of 0.04. We consider $\rho_i/\rho_e=5$ and for zero twist the ratio of Alfvén speeds $V_{ae}/V_{ai}=3$. Hence the ratio $B_e^2/B_i^2 = 1.8$. In the transition region (where the gradient is sharp) which spans over one or two cells horizontally this ratio changes slightly. Nonzero values of B_{0z} cause the appearance of additional local extrema in the Alfvén speed. These extrema become much pronounced for larger twist. As a result of these extrema wave trapping is also possible at the slab edges and, consequently, fine structures can occur.

3 Simulation model

The numerical simulations were performed with a 2.5 dimensional resistive MHD code. The code uses the well-known flux-corrected transport (FCT for brevity) technique (Devore, 1991, 1994; Murawski and Goossens, 1994b; Murawski et al 1996). The details about the code are given in Parhi *et al.*, 1996.

The computational box $(-5a, 5a) \times (-8a, 8a)$ consists of 100 cells in both horizontal x and vertical y directions. This roughly corresponds to 10^4 km horizontally and 16×10^3 km vertically. We consider free-slip, rigid wall boundary conditions at the top and bottom of the simulation regions ($y = \pm 8a$): $V_y = 0$ and $\partial f / \partial y = 0$ for $f = \rho, p, B, V_x$, and V_z . This appears to be a reasonable constraint because the motions in the solar corona cannot much effect the high density photosphere. At the remaining (x) boundaries we applied open (zero gradient) conditions for all of the variables.

We study the effect of photospheric footpoint motions. Thus, at the bottom of the simulation region we impose a body force F_z as follows:

$$F_z(x, y = -8a, t) = F_d(x) \sin(\omega_d t),$$

$$F_d(x) = \begin{cases} F_d, & |x| \leq a, \\ F_d / \cosh^{14}(|x| - a), & |x| > a. \end{cases}$$

Here, the constant F_d is the amplitude of the driver and ω_d is the driving frequency.

4 Results

We analyze in this paper the effect of equilibrium sheared flow on the resonance heating of the coronal loop by the plasma waves. The two-dimensional equilibrium flow components V_x and V_y are proportional to $B_{0y}(x)$ and the proportionality constant V is assumed to be 0.1 for V_y and 0.01 for V_x . Thus $\hat{V}_x = 0.01V_{ae}$ and $\hat{V}_y = 0.1V_{ae}$ where V_{ae} is the Alfvén velocity at the edge of the slab. First we study the effect of vertical non-zero flow (i.e. $V_y \neq 0$), and subsequently a small horizontal (i.e., V_x) component of the flow is introduced. We collect from previous simulation results (Parhi et al., 1996) that for zero or small twist ($c \leq 0.03V_{ae} \sqrt{\mu\rho_e}$) waves are excited preferably as sausage modes. The contour plot of V_x at $t = 300L/V_{ae}$ indicate that the waves develop kink instability in the upper part of the loop (not shown). Figure 1 describes a situation where $\hat{V}_x = 0.0$ and

$\hat{V}_y = 0.1V_{ae}$ at time $t = 177L/V_{ae}$. We see some signature of kink instability and traces of logarithmic singularities. For a right kind of frequency of the driver it is known that the magnetosonic waves exhibit logarithmic singularity. However, we note that this feature is not very prominent compared with that at earlier time (Parhi et al., 1996) because due to finite resistivity the singularity smoothens after $t > t_c$ where $t_c \sim \eta^{-1/3}$. Further temporal evolution (till $t = 300L/V_{ae}$) completely removes the singularity. Thus we infer that the flow inhibits the development of kink instability. Further, the surface plot corresponding to the contour plot for $t = 300L/V_{ae}$ did not show any trace of singularity implying the flow is uniformly heating the plasma. As mentioned earlier, Hollweg et al. (1990) have concluded that under certain conditions flow facilitates heating. Perhaps, we are observing the same effect here numerically.

In the absence of equilibrium flow, the velocity profiles for slow mode waves (Murawski et al., 1996 and references therein) do not remain symmetric in x when twist $c = 0.6V_{ae}\sqrt{\mu\rho_e}$ is included. This was also noticed by Parhi et al. (1996). The vortex-like structures initially formed at the bottom of the coronal loop appeared to diffuse to the top of the loop. The above transition from organised structures to disorganized ones could be related to the ongoing convective processes at the photosphere. The inclusion of a slight y-component of velocity, $\hat{V}_y = 0.1V_{ae}$ (Figure 2 taken at $t = 177L/V_{ae}$), has tremendous effect on the evolution of waves. From Figure 2 we notice that the flow has a tendency to diverge towards the end of the loop. The rigid wall boundary conditions prevents the flow to penetrate into the top boundary and hence the plasma tends to spread near the top. The steep profiles for density and magnetic field orients the flow in such a manner that it concentrates on the specific layers. As time evolves (i.e., at $t = 300L/V_{ae}$) the spreading of plasma near the top boundary ceases (not shown). Rather the two concentrated layers get separated in the middle of the loop and subsequently get closer near the top boundary . Some vortex like stuctures reappear at the footpoints.

When a small non-zero x-component of velocity, $\hat{V}_x = 0.01V_{ae}$, is included in addition

to $\hat{V}_y = 0.1V_{ae}$, the velocity profiles undergo drastic changes. It helps to smooth out the existing gradients which can even be located in the velocity structures extending to the far left. The center of the loop appears to consist of elongated plasma vortices (not shown) which suggest that it may ultimately break down with further evolution. From this, we conclude that the presence of equilibrium flow facilitates the stretching of vortices.

Now we will discuss $V_3 = (B_{0y}V_z - B_{0z}V_y)/(B_{0y}^2 + B_{0z}^2)^{1/2} \approx V_z$ which is roughly associated with Alfvén waves (Erdélyi and Goossens, 1994). The plots of V_3 at $t = 300L/V_{ae}$ in the absence of equilibrium flow (not shown) indicate the formation of dense elongated Alfvén vortices near the top left edge of the boundary surrounded partially by rarefied smooth plasma zones. When small non-zero y-component of the equilibrium flow is present (Figure 3), we see at $t = 177L/V_{ae}$ the formation of dense elongated vortices at various heights of the loop. The whole contour picture can be considered consisting of two large half open vortices engulfing many closed ones indicating the localised deposition of wave energy. The microstructure are the possible signature of the direct cascade of energy from large to small scale length. As time evolves a snap shot at $t = 300L/V_{ae}$ (not shown) indicates no vortex implying that the flow has uniformly heated the plasma. When small non-zero x-component of velocity is introduced some of the vortices reappear in the middle of the slab with the larger concentrated ones forming canal like features (not shown). Thus introduction of a small x-component of velocity preferentially builds up the storage of wave energy in the center of the simulation box. The imposed boundary conditions apparently play a great role in the development of velocity structures.

The Ohmic heating (ηj^2) profile at $t = 300L/V_{ae}$ for the case of no equilibrium shear flow show a sharp peak at the left edge. This could be due to resonance heating of Alfvén waves. Also if one compares these profiles with plots of V_3 , then the correlation between vortex formation and heating patterns becomes apparent. When a small shear flow in y-direction is included (Figure 4) the pattern of heating completely changes. The flow brings in more or less symmetric distribution of heating. It is natural to think that the

flow changes the condition of resonance. Comparing Figure 3 with the heating contours (Figure 4), the relation between the vortex structures and Ohmic heating becomes clear. When the plasma evolves for longer time the heating becomes uniform. When little x-component of velocity is included the heating pattern becomes symmetric confirming the vortex picture (not shown) where large canals of plasma were observed. Two clear layers of concentrated heating are visible. The width of these layers is larger in comparison with that of the resonance layer when there is no flow or only flow in y-direction (Figure 4). Thus x-component of velocity enhances the occurrence of resonance which in turn promotes more heating, This could probably explain the heating of the solar corona in general because in reality V_x and V_y should be present.

5 Conclusion

In our simulations the periodic driver, which mimics the foot point motions in the photosphere, leads to the generation of MHD waves in the coronal loops. The signature of kink instability and traces of logarithmic singularities disappear as time progresses suggesting that the flow inhibits the kink mode. The flow has a dramatic effect on resonance heating as manifested by large changes in vortex structures. The flow brings more or less symmetric distribution of heating. The center of the coronal loop consists of elongated plasma vortices suggesting that the further evolution may lead to its break-down. The resultant microstructure are the possible signature of the self organisation implying the direct cascade of energy from large to small scale lengths. There exists a correlation between vortex formation and heating pattern.

Acknowledgements

Some of this research was performed at the Jet Propulsion Laboratory, California Institute of Technology, Pasadena under contract with the National Aeronautics and Space Administration. G S Lakhina wishes to thank the National Research Council for the award of a Senior Resident Research Associateship at the Jet Propulsion Laboratory.

REFERENCES

- Cadez, V. M. and Ballester, J. L.: 1994, *Astron. Astrophys.*, in press.
- Choudhuri, A. R., Auffret, H. and Priest, E. R.: 1993a, *Solar Phys.* 143, 49.
- Choudhuri, A. R., Dikpati, M. and Banerjee, D.: 1993b, *Astrophys. J.* **413**, 811.
- DeVore, C. R.: 1991, *J. Comp. Phys.* 92, 142.
- DeVore, C. R.: 1994, *Flux-corrected transport modules for solving multidimensional compressible magnetohydrodynamics problems on parallel computers*, Naval Research Laboratory Memorandum Report, in preparation.
- Erdélyi, R. and Goossens, M.: 1994, *Astrophys. Space Sci.* 213, 273.
- Goedbloed, J. P.: 1983, *Lecture Notes on Ideal Magnetohydrodynamics*, Rijnhuizen Report 83-145, Nieuwegein, The Netherlands.
- Goossens, M.: 1991, in E. R. Priest and A. W. Hood (eds), *Advances in Solar system Magnetohydrodynamics*, Cambridge Univ. Press, Cambridge, p. 137.
- Goossens, M., Ruderman M. and Hollweg, J. V.: 1995, *Solar Phys.*, 157, 75.
- Hollweg, J. V.: 1981, *Solar Phys.* 70, 25.
- Hollweg, J. V.: 1990, *Comp. Phys. Rep.* 12, 205.
- Hollweg, J. V., Yang G., Cadez, V. M. and Gakovic, B. 1990, *Astrophys. J.* 349, 335.
- Hollweg, J. V.: 1992, *Astrophys. J.* 389, 731.
- Ionson, J. A.: 1978, *Astrophys. J.* 226, 650.
- Karpen, J. T., Antiochos, S. K. and DeVore, C. R.: 1991, *Astrophys. J.* 382, 327.

- Murawski, K. and Goossens, M.: 1994a, *Astron. Astrophys.* 286,952.
- Murawski, K. and Goossens, M.: 1994b, *Astron. Astrophys.* 286,943.
- Murawski, K., DeVore, C. R., Parhi, S. and Goossens, M.: 1996, *Planet Space Sci.* 44,
- Parhi, S., De Bruyne P., Murawski, K., Goossens, M. and DeVore, C. R.: 1996, *Solar phys.*, V
- Parhi, S., Pandey, B. P., Goossens, M., Lakhina, G. S. and De Bruyne P. : 1996, *Adv. Space Sci.*, in press.
- Parhi, S., Pandey, B. P., Goossens, M., Lakhina, G. S. and De Bruyne P. : 1997, *Astro. Space Sci.*, submitted.
- Priest, E. R.: 1981, in E. R. Priest (ed), *Solar Flare Magnetohydrodynamics*, Gordon and Breach Science Publishers, New York.
- Yang G. and Hollweg, J. V.: 1991, *J. Geophys. Res.* 96, 13807.

Figure Captions

Fig. 1: Spatial variation of V_x at $t = 177 L/V_{ae}$ in the presence of equilibrium $\hat{V}_y = 0.1V_{ae}$.

Fig. 2: Spatial variation of V_y (corresponding to slow waves) at $t = 177 L/V_{ae}$ in the presence of equilibrium $\hat{V}_y = 0.1V_{ae}$.

Fig. 3: Spatial variation of V_3 (corresponding to Alfvén waves) at $t = 177 L/V_{ae}$ in the presence of equilibrium $\hat{V}_y = 0.1V_{ae}$.

Fig. 4: Spatial variation of J^2 (corresponding to Ohmic heating) at $t = 177 L/V_{ae}$ in the presence of equilibrium $\hat{V}_y = 0.1V_{ae}$.

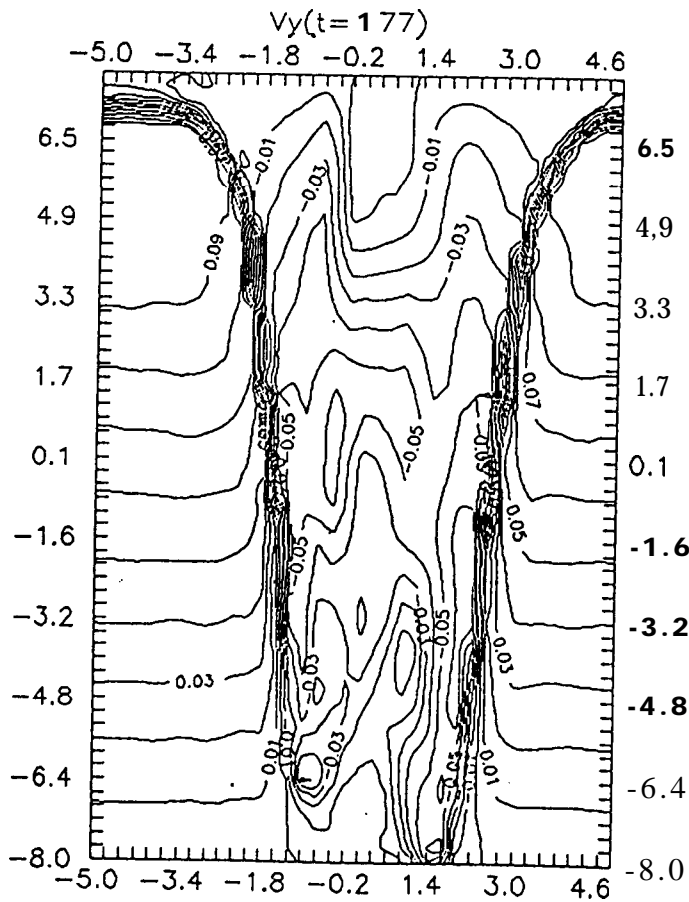
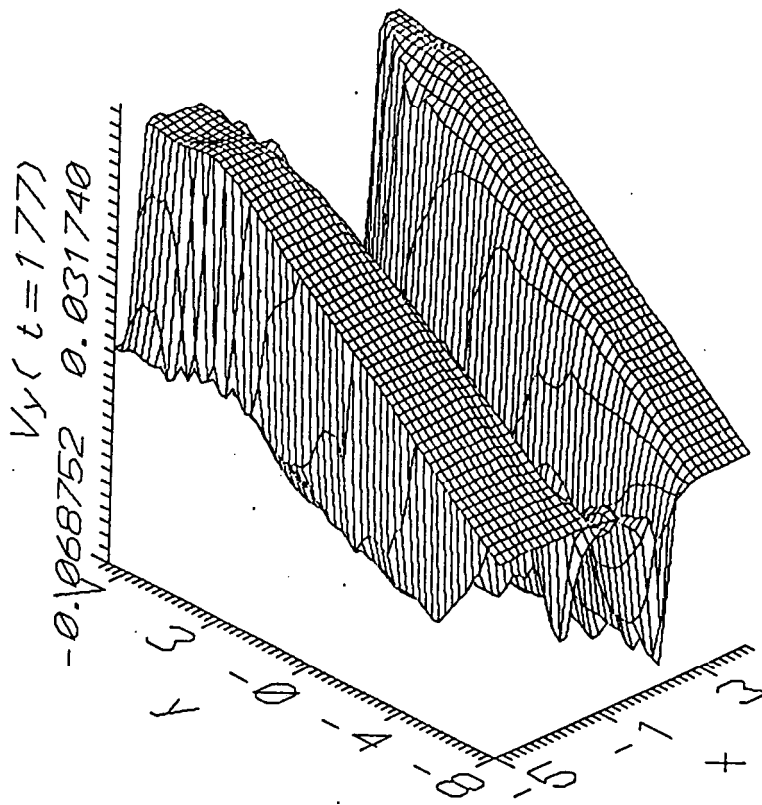


Fig. 2

